High-pressure CO_2/CH_4 separation of Zr-MOFs based mixed matrix membranes

Mohd Zamidi Ahmad[1,2,3], Thijs A. Peters[4], Nora M. Konnertz[5], Tymen Visser[5], Carlos Téllez[3], Joaquín Coronas[3], Vlastimil Fila[1], Wiebe M. de Vos[2], Nieck E. Benes[2*]

[1]Department of Inorganic Technology, University of Chemistry and Technology, Technicka 5, Dejvice – Praha 6, 16628 Prague, Czech Republic

[2]Membrane Science and Technology, Faculty of Science and Technology, MESA+ Institute for Nanotechnology, University of Twente, P.O. Box 217, AE Enschede, Netherlands

[3]Chemical and Environmental Engineering Department and Instituto de Nanociencia de Aragón (INA), Universidad de Zaragoza, 50018 Zaragoza, Spain

[4]SINTEF Industry, P.O. Box 124 Blindern, N-0314, Oslo, Norway

[5]European Membrane Institute Twente (EMI), Faculty of Science and Technology, University of Twente, P.O. Box 217, AE Enschede, Netherlands

*Corresponding author: n.e.benes@utwente.nl

Abstract

The gas separation properties of 6FDA-DAM mixed matrix membranes (MMMs) with three types of zirconium-based metal organic framework nanoparticles (MOF NPs, ca. 40 nm) have been investigated up to 20 bar. Both NPs preparation and MMMs development were presented in an earlier publication that reported outstanding CO_2/CH_4 separation performances (50:50 vol.% CO_2/CH_4 feed at 2 bar pressure difference, 35 °C) and this continuation study is to demonstrate its usefulness to the natural gas separation application. In the current work, CO_2/CH_4 separation has been investigated at high pressure (2 – 20 bar feed pressure) with varying CO_2 content in the feed (10 – 50 vol.%) in the temperature range 35 – 55 °C. Moreover, the plasticization, competitive sorption effects, and separation of the acid gas hydrogen sulfide (H_2S) has been investigated in a tertiary feed mixture of CO_2:H_2S:CH_4 (vol.% ratio of 30:5:65) at 20 bar and 35 °C. The

incorporation of the Zr-MOFs in 6FDA-DAM enhances both CO_2 permeability and CO_2/CH_4 selectivity of this polymer. These MMMs exhibit high stability under separation conditions relevant to an actual natural gas sweetening process. The presence of H_2S does not induce MMM plasticization, but only causes reversible competitive sorption that reduces the CO_2/CH_4 selectivity with only 17 – 19% as compared to 30% for the neat membrane. The overall study suggests a large potential for 6FDA-DAM Zr-MOF MMMs to be applied in natural gas sweetening, with good performance and stability under the relevant process conditions.

Keywords: Zr-based MOF, mixed matrix membrane, high-pressure separation, CO_2 capture, H_2S.

1.0. INTRODUCTION

The acid gas content (carbon dioxide, CO_2; hydrogen sulfide, H_2S) in raw natural gas varies accordingly to the hydrocarbon geo-origins [1–3] and is commonly in the range of 25 – 55 mol.% for CO_2 and below 2 mol.% for H_2S (≥ 5 mol.% in several regions) [4–6]. CO_2, the most undesirable diluent aside from H_2S, is essential to be discarded from the gas stream as it corrodes transmission pipelines in the presence of water [7,8]. Additionally, CO_2 lowers the natural gas caloric value and causes atmospheric pollution [3,4,7,8]. Consequently, the content of impurities must be reduced to meet the industrial processing and pipeline distribution requirements, e.g., maximum allowable contents of 2 – 3 mol.% CO_2 and 0.0004 – 0.0005 mol.% (4.3 – 5.0 ppm) H_2S (see Table S1) [9]. In the last decades, the advances in gas separation membranes have allowed the technology to increase its share of the total membrane market, comprising over 1,000 – 1,500 million US dollar per year [10] and appear to be the most viable alternative to substitute current energy driven processes, including the solvent-based adsorption processes [7,13]. However, due

to challenges such as plasticization especially at high-pressure operation and degradation, membrane processes only represents <5% of the natural gas sweetening market [11,12].

Both plasticization and degradation effects can be suppressed by polymer blending and cross-linking [14–17], but a more promising method to provide these advantages is the combination of polymeric and inorganic materials as mixed matrix membranes (MMMs) [18–21]. In addition to 40.8% CO_2 permeability and 11.4% CO_2/CH_4 selectivity improvements, Yong *et al.* [18] also reported the effectiveness of 2 wt.% POSS (polyhedral oligomeric silsesquioxane) nanoparticles into the highly permeable PIM-1. They also suppressed the neat polymer CO_2-induced plasticization pressure of 15 bar in the range of tested pressure (30 bar) with 50:50 vol.% CO_2:CH_4 feed mixture, at 35 °C. Adams *et al.* [19] reported a more than five times increase of CO_2 partial pressure needed to plasticize PVAc-50 wt.% zeolite 4A at 30 bar, also measured with 50:50 vol.% CO_2:CH_4 feed mixture, at 35 °C. Both Shahid and Nijmeijer [20] and Samadi and Navarchian [21] reported higher CO_2-plasticization pressures of Matrimid® 5218 (neat $P_{plasticization.}$ of ~10 bar) by incorporating 30 wt.% mesoporous Fe-BTC [20], 5 wt.% MgO [21] and 10 wt.% modified clay mineral with polyaniline [21], up to 21, 15 and 30 bar, respectively.

Permeation of a mixture of gases through a membrane can depend strongly on the operating parameters, for example the feed pressure and temperature, due to the gases non-ideal behavior [22–24] and their competitive sorption [22,24–26]. Moreover, in a MMM system, the presence of a porous filler and the new filler-polymer interfacial phase created need to be understood as they further influence the gas mobility and sorption through the membrane. Metal organic frameworks (MOFs), formed with metal-based clusters linked by organic ligands [27] in three-dimensional crystalline frameworks with permanent porosity, are an emerging class of porous fillers [28]. They have gained substantial attention due to their high CO_2 uptake (i.e., HKUST-1 of 7.2 $mmol \cdot g^{-1}$

[29], MOF-74 of 4.9 mmol·g^{-1} [30], at 1 bar, 273 – 298 K), large surface areas up to 7000 m^2·g^{-1} [31], well-defined selective pores due to their crystallinity and many MOFs show superior thermal and chemical stability [32], amongst other features. Many researchers observed that the incorporation of a MOF into the polymer continuous phase not only improved its separation properties but also its physical properties [18,33–35], due to their excellent interfacial reaction where the polymer adapt to the morphology offered by the MOFs. The polymer in some cases penetrate into the MOF open pores or rigidifies and forms microvoids at the interface [36,37], simultaneously affecting the membrane's physical properties and gas separation performance.

Zr-based MOF UiO-66 is a highly stable new material and has recently been applied as part of a MMM [33,38,39]. The synthesis of three types of Zr-MOFs, namely UiO-66 and its functionalized derivatives, UiO-66-NH_2 and UiO-66-NH-$COCH_3$, as well as MMM fabrication with 6FDA-DAM have been presented earlier [36,40]. In the current paper, we present the gas separation performance of the neat 6FDA-DAM membranes and their derived Zr-MOF MMMs as a function of feed pressure between 2 and 20 bar. At the highest pressure, the effects of CO_2 content in the feed mixture on membrane performance has been investigated, at various temperatures (35 – 55 °C). Finally, the presence of H_2S to the separation performances is studied.

2.0. EXPERIMENTAL

2.1. Materials and membrane fabrications

The UiO-66 and UiO-66-NH_2 NPs (ca. 40 nm in size) were synthesized accordingly to Hou *et al.* [40], at 1 to 1 molar ratio of zirconium (IV) chloride ($ZrCl_4$, ≥99.5% trace metal basis) to 1,4-benzenedicarboxylic acid (BDC, 98%) or 2-amino-1,4-benxenedicarboxylic acid (NH_2-BDC, 99%), in *N,N*-dimethylformamide (DMF, ≥99.9%), through a solvothermal process in a pre-heated

oven at 120 °C during 24 h for UiO-66 and at 80 °C during 14 h for UiO-66-NH_2. A second heating step was conducted for UiO-66-NH_2 at 100 °C for 24 h. UiO-66 was activated by thermal treatment in a furnace at 300 °C for 3 h, with a heating rate of 15 °C·min^{-1}, whereas chemical activation was conducted for UiO-66-NH_2, where the precipitated NPs were washed in an absolute ethanol bath at 60 °C, three times in three days (ethanol was changed daily). After the complete cycle, the NPs were dried at room temperature. A covalent post-synthetic modification (PSM) was conducted onto UiO-66-NH_2 to produce UiO-66-NH-$COCH_3$ in chloroform ($CHCl_3$, anhydrous ≥ 99%) and acetic anhydride (AcO_2, ACS Reagent, ≥98.0%) solution, under reflux at 55 °C / 24 h. Once completed, the colloidal solution was centrifuged, rinsed with fresh $CHCl_3$ (15 mL, 3x) and dried overnight at 150 °C before characterization and use. The conversion yield was determined by the percentage of amide groups present in the modified NPs using proton nuclear magnetic resonance (^{1}H NMR), and the digestion method was presented elsewhere [40,41]. All reactants applied in the NP synthesis were supplied by Sigma-Aldrich.

6FDA-DAM (Mw = 418 kDa) was purchased from Akron Polymer Systems, Inc. and dried overnight at 100 ºC before use. Pure polymer membranes ("neat") and MMMs were fabricated by dissolving the corresponding amount of 6FDA-DAM in chloroform, making a dope solution of 10 wt.%. In the case of MMM, a priming step was conducted with 10 – 15 wt.% of the total polymer weight that proves to improve the inorganic filler dispersion in the continuous polymer phase [42–44]. The final dope solutions were casted in a Petri dish and covered for controlled solvent evaporation overnight before being treated at 110 °C before subsequent characterization and permeation measurements. The flat sheet membranes were in the thickness range of 100 – 150 μm.

2.2. Standard permeation measurement

To assess the gas separation performance of the membranes, a 25/25 $cm^3(STP)\cdot min^{-1}$ CO_2/CH_4 binary feed mixture was used at a pressure difference of 2 bar at 35 ºC applying He as sweep gas at 1 cm^3 $(STP)\cdot min^{-1}$. The permeate composition was analyzed online by an Agilent 3000A micro-GC equipped with a thermal conductivity detector (TCD) at the Institute Nanoscience of Aragon (INA), University of Zaragoza. The membrane module is as described elsewhere [45]. The permeability was calculated as the penetrated gas flux, normalized for the membrane thickness and the partial pressure drop across the membrane, and presented in Barrer (1 Barrer = 10^{-10} $cm^3(STP)\cdot cm\cdot cm^{-2}\cdot s^{-1}\cdot cmHg^{-1}$ (Eq. 1).

$$Permeability, P_{gas} = \frac{Flux_{gas}\left(cm^3(STP).cm^{-2}.s^{-1}\right)\times Thickness\ (cm)}{\Delta p_{gas}\ (cm.Hg)} \quad \text{Eq. 1}$$

The separation factor (α) of two competing gases was calculated using Eq. 2, considering the mole fraction (x) of gas i and j in both feed and permeate streams. The mixed gas separation performance was previously discussed [36] and the best performing MMMs with 14 – 16 wt.% Zr-MOF particle loadings.

$$\alpha_{i/j} = \frac{x_i^{perm.}/x_j^{perm.}}{x_i^{feed}/x_j^{feed}} \quad \text{Eq. 6-2}$$

2.3. High-pressure performance evaluation

The membranes were placed in a proprietary high-pressure permeation module obtained from the European Membrane Institute (EMI, The Netherlands). The membrane was supported with an S&S 589/1 black ribbon ash-less filter paper on a perforated plate to avoid membrane deformation during the high-pressure testing. The sample was sealed with an o-ring system providing for an effective membrane area of 0.78 cm^2. Both feed and retentate sides were connected by high-

pressure Swagelok quick-connects whereas the permeate gas was collected using a 1/8 inch Swagelok connector.

The permeation module was placed inside a Memmert UF450 forced air circulation oven, connected to a proprietary permeation set-up at SINTEF Materials and Chemistry, Oslo for high-pressure gas separation measurement (Fig. 1). The permeation set-up is designed to withstand pressures up to 92 bar with a forced air temperature control up to 300 °C. The feed (150 $cm^3(STP)\cdot min^{-1}$) and permeate (10 $cm^3(STP)\cdot min^{-1}$) flow rates were controlled by automated Bronkhorst High-Tech mass controllers (MFC), equipped with a back pressure controller (Bronkhorst High-Tech, P-512C equipped with an F-033C control valve, max of 92 bars) on the feed side for pressure regulation. The atmospheric-pressure permeate gas analyzed by a two-channel column (MolSieve 5A, MS5 and PoraPLOT U, PPU) Agilent 490 micro-GC, coupled with thermal conductivity detectors (TCD). The micro-GC was calibrated for low CO_2 (0 – 12 vol.%), CH_4 (0 – 5 vol.%) and H_2S (0 – 0.5 vol.%) concentrations in argon. Good correlation coefficients of $R^2 = \geq 0.999$ were obtained for the μ-GC response as a function of CO_2, CH_4, and H_2S concentration. The fluxes were calculated from the measured permeate concentrations and the calibrated flow of Ar sweep gas.

High-pressure gas permeation measurements were conducted to the following experimental sequence, and the separation performances were calculated correspondingly to Eq. 1 and Eq. 2.

1. Pressure variation with 50 vol.% CO_2 in the feed content: Preliminary measurement with a 50:50 vol.% CO_2: CH_4 feed mixture (at 2 bar, 35°C) was conducted to validate the initial membrane performances, and the pressure was subsequently increased to 5 and 10 bar. Before proceeding to 20 bar, the CO_2 feed content was decreased to 10 vol.% for the second step measurements.

2. CO_2 feed content variation at the feed pressure of 20 bar: At 20 bar, the 10 vol.% CO_2 feed content was subsequently increased to 20 vol.%, 30 vol.%, and 50 vol% with CH_4.
3. The effect of temperature variation on the separation performance, with 30:70 vol.% CO_2:CH_4 feed mixture at 20 bar: The temperature increase was conducted by stepwise increments from 35 °C to 45 °C and 55 °C, and followed by a reduction back to 35 °C prior to the H_2S introduction (step no. 4).
4. Investigation of separation performance in the presence of H_2S with 30:5:65 vol.% CO_2:H_2S:CH_4 feed mixture was conducted at 20 bar and 35 °C.

It is important to note that the samples were allowed to equilibrate overnight, after each pressure or feed composition change. Specific attention was given to Health, Safety and Environmental (HSE) matters, and the lab was equipped with preventive safety measures which include H_2, CO, and H_2S detection systems, personal portable gas detectors, and separate floor level ventilation suction.

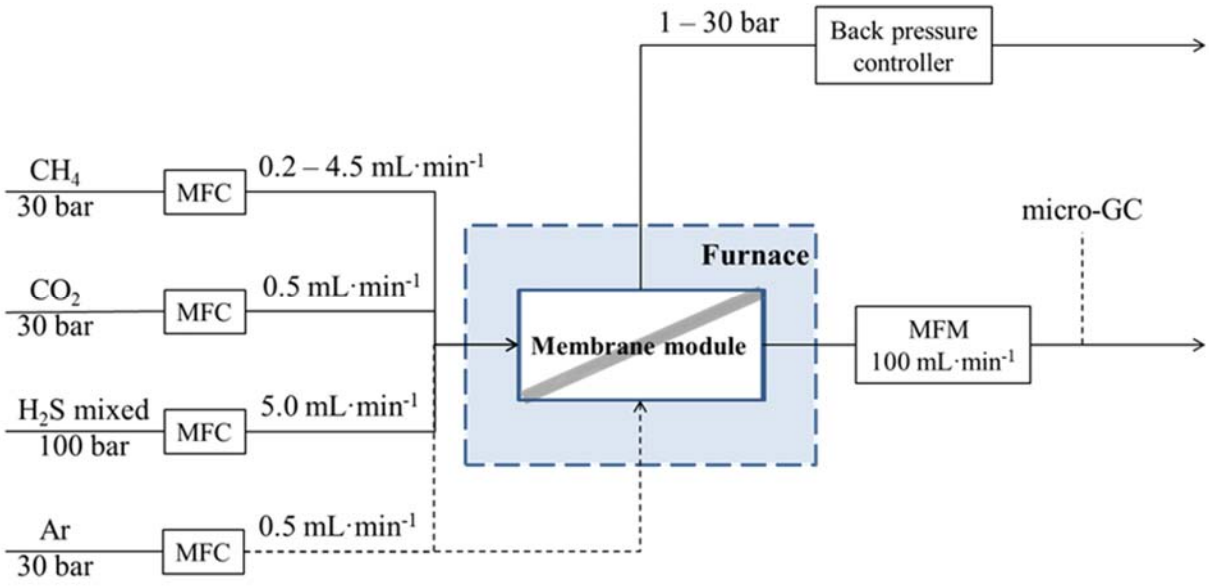

Fig. 1: Schematic representation of the high-pressure experimental set-up.

3.0. RESULTS AND DISCUSSIONS

In the previous publication [36], we found very promising performance indicators for several 6FDA-DAM MMMs with Zr-MOFs when tested at low pressure (2 bar), with the best performance observed for membranes that contain 14 – 16 wt.% Zr-MOF. An increase in the Zr-MOF loading shows a clear permeability-selectivity trade-off and selectivity reductions have been observed [36,46]. Table 1 shows the re-measured gas separation performance of the duplicate membranes, at 35 °C, with a pressure difference of 2 bar with an equimolar binary mixture of CO_2 and CH_4. The values are highly compliance with the published data and similar improvement behaviors were observed. The presence of 14 wt. % UiO-66, 16 wt. % UiO-66-NH_2 and 16 wt. % UiO-66-NH-$COCH_3$ improves the CO_2 permeability of 6FDA-DAM (P_{CO2} = 335 Barrer) by 165%, 56% and 37%, respectively. These enhancements are well-related to the CO_2-philic nature of the Zr-MOFs where a stronger energetic interaction between CO_2 (higher quadrupole moment than CH_4) and the nanoparticle surfaces at zero coverage, and to the increments in free fractional volume (FFV) in the MMMs (Neat 6FDA-DAM, FFV = 0.238). 14 wt. % UiO-66 MMM presents the highest value of 39%, followed by 16 wt. % UiO-66-NH_2 and 16 wt. % UiO-66-NH-$COCH_3$ with 16% and 22%, respectively. The CO_2/CH_4 selectivity of the samples also increased by 23 – 32%.

At these observed optimum loadings the Zr-MOFs addition enhances both CO_2 permeability and CO_2/CH_4 selectivity to beyond the permeability-selectivity trade-off [46]. Besides a higher gas diffusion in the Zr-MOFs, the NPs addition improved the MMM gas diffusivity by inducing an ancillary selective interface phase [47] with additional free volume [48,49]. Agglomeration of the NPs was more prominent at the highest loadings, and the concurrent reduction of the selectivity reduction is likely due to the formation of non-selective by-pass channels in the filler agglomerates

[48] and possibly micro-voids in the filler-polymer interface region [43], although such morphological features are not observed by SEM analyses.

Table 1: CO_2 and CH_4 permeability and CO_2/CH_4 selectivity of the neat 6FDA-DAM and its Zr-MOF MMMs, measured 35 °C, at a pressure difference of 2 bar with an equimolar binary mixture of CO_2 and CH_4

Membrane	**Gas permeability (Barrer)**		**CO_2/CH_4 Selectivity**
	CO_2	**CH_4**	
Neat	335	17.7	19.3
MMM UiO-66 14 wt.%	888	35.9	25.1
MMM UiO-66-NH_2 16 wt.%	521	21.9	23.8
MMM UiO-66-NH-$COCH_3$ 16 wt.%	459	18.1	25.4

3.1. Effect of feed pressure to mixed gas separation

Most of the fundamental studies on Zr-MOF polyimide MMMs have been conducted at low pressures and therefore it lacks investigation of CO_2-induced plasticization, related to Matrimid and 6FDA-copolyimides [33,50,51]. Here, we have investigated the gas separation performance of 6FDA-DAM and its Zr-MOF MMMs at a pressure ranging between 2 to 20 bar in a 50:50 vol. % CO_2:CH_4 feed mixture at 35 °C. The obtained mixed gas permeability and CO_2/CH_4 selectivity behavior as a function of pressure are shown in Fig. 2.

The CO_2-induced plasticization pressure is defined to occur at the minimum observed in the CO_2-permeability as a function of CO_2-partial feed pressure. In the case of mixed gases, the permeation rate of all gases is affected due to swelling of the polymer matrix and the increased chain mobility caused by the high CO_2 concentration. The enhancement in permeation is more pronounced for the least permeable gases, resulting in a decrease of the selectivity as a function of

pressure. In contrast, for all samples in the present study, a monotone decrease in CO_2 permeability with increasing pressure is observed (See Fig. S1), which does not indicate substantial plasticization [22]. The decrease in CO_2 permeability reduction is a result of competitive sorption. The corresponding concave shape of the sorption isotherm [26,52] constitutes a reduction in driving force for transport with increasing pressure and, in addition, gradual saturation of the material may result in lower mobility (decreasing diffusion and permeation coefficient in the membrane matrices) (see Fig. S1). The CO_2 permeability continuous decreases with increasing pressure indicate the dominance of dual-mode adsorption [22,53] and show the absence of CO_2-induced plasticization in the thick membrane [22], opposite to the reported single-gas CO_2-plasticization pressure of neat 6FDA-DAM membrane between ~ 10 – 20 bar, at 35 °C [54,55]. The plasticization pressure differences may be attributed to different physical properties, i.e., molecular weight, density and polymer free volume, as previously discussed [33,36]. In any event, as the current highest CO_2 partial pressure in the feed was 10 bar (20 bar of feed total pressure with 50% CO_2), the conditions would not be favorable to observe plasticization.

The pressure dependence of the CH_4 permeability (Fig. 2 (b)) over the measured pressure range, however, suggest that the neat 6FDA-DAM and UiO-66-NH_2 MMM starts to swell immediately after the first pressure increment. The phenomenon, to the function of pressure, causes a higher successful jump into a free volume thus increases the low permeating component's mobility (CH_4), making the effect more apparent while simultaneously reduces the successful jumps percentage of the higher permeating component (CO_2) into the same free volumes. Even though this was not yet the plasticization pressure as CO_2 permeability continued to decrease, their CO_2/CH_4 selectivity reduced by 55% and 58% respectively. The reduction is probably due to the larger decrease in the CO_2 solubility coefficient compared to CH_4 [56]. Heck *et al.* [57] observed

similar behavior in (6FDA-mPDA)-(6FDA-durene) block co-polyimide, for which they reported an increase in CH_4 permeability with pressure (up to 20 bar feed pressure), causing CO_2/CH_4 and He/CH_4 selectivity reductions. The behavior was defined as swelling-induced perm-selectivity losses, which was also observed in several other co-polyimides, such as 6FDA-APAF and TPDA-APAF, when measured with CO_2/CH_4 binary mixture up to 25 bar feed pressure, at 35 °C [58]. The continuous decrease of CH_4 permeability in both UiO-66 and UiO-66-NH-$COCH_3$ MMMs demonstrated the competitive sorption effect [59], where CO_2 penetrated into the membranes' sorption sites which associated to the non-equilibrium free volume in glassy polymer and hindered CH_4 to permeate. Polymer plasticization was not observed in these membrane samples.

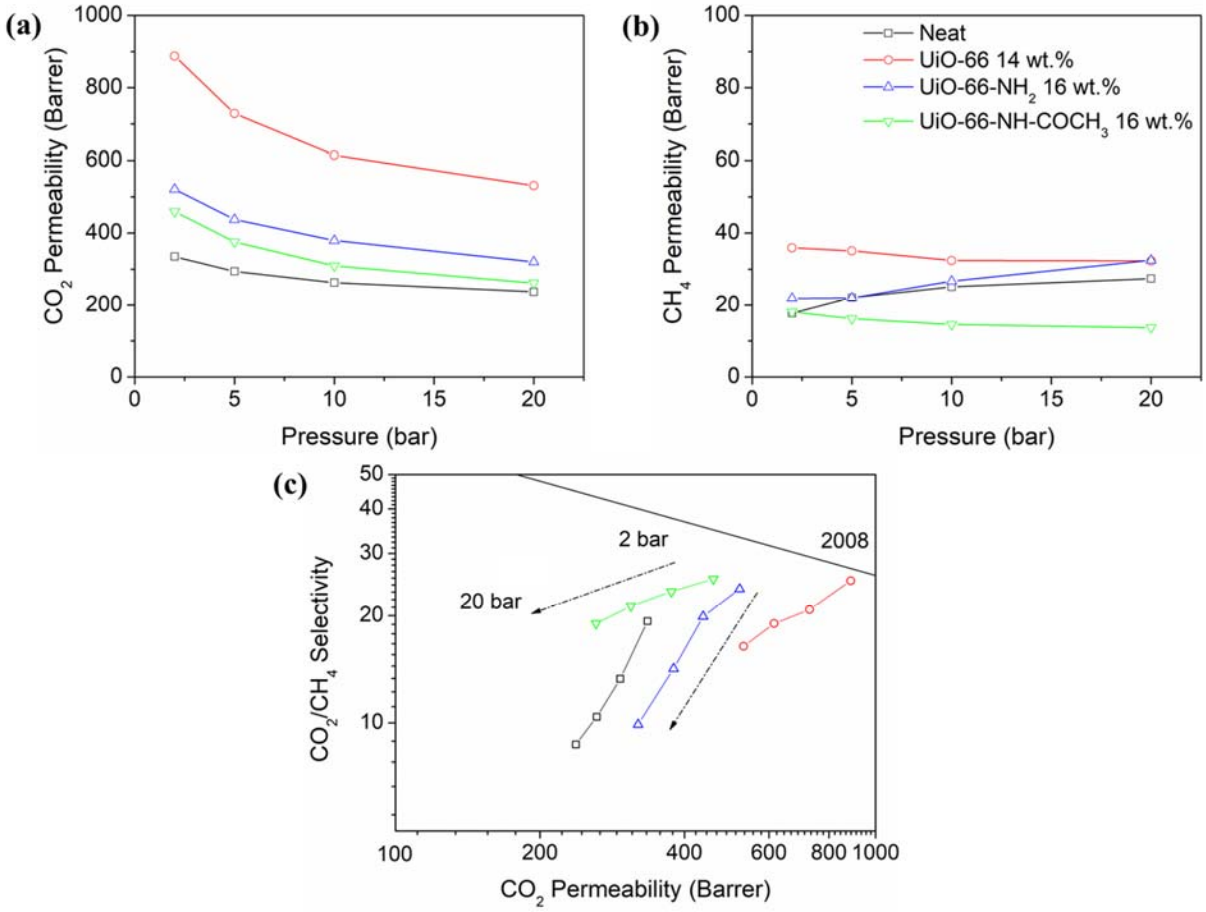

Fig. 2: (a) CO_2 and (b) CH_4 permeabilities of 6FDA-DAM and its Zr-MOFs as a function of feed pressure, measured with 50:50 vol.% CO_2: CH_4 feed mixture at 35 °C. Their corresponding CO_2/CH_4 selectivity values are presented in (c), against the 2008 Robeson upper bound [60].

3.2. Effect of CO_2 feed composition in high-pressure separation

Fig. 3(a) and 3(b) show the CO_2 and CH_4 permeability of the neat 6FDA-DAM and Zr-MOF MMMs, measured at 20 bar feed pressure and 35 °C, with a varying CO_2 feed content between 10 to 50 vol.%. The CO_2 permeability decreases for the neat 6FDA-DAM and its Zr-MOF MMMs, with an increase of the CO_2 content between 9 and 22%, with the lowest reduction observed for the UiO-66 MMM. The observation, however, is opposite to the previously reported CO_2 permeability relationship with CO_2 partial pressure at low-pressure measurements, i.e., 6FDA-

DAM Zr-MOF MMMs (at 2 bar) [36] and PES/SAPO-34/2-hydroxyl 5-methyl aniline MMMs (at 3 bar) [61]. At the low pressure, a higher CO_2 partial pressure produced a more prominent competitive sorption effect, where an increase in CO_2 solubility and transport through the membrane medium was observed and inversely decreased the second component's ability to permeate, in this case, CH_4.

Evidently, the continuous CO_2 permeability reduction with increasing pressure suggests that the competitive sorption effect at high pressure is less influenced by the CO_2 partial pressure (see Fig. S2). Instead, it is merely related to gradual saturation of the permeating gases inside the polymer micro-voids [20]. Nevertheless, a slight increase in the CH_4 permeability for the neat membrane (9%) and UiO-66-NH_2 MMM (21%) is observed, indicating the possibility of CO_2-induced plasticization that started to take effect [62,63]. These samples exhibited the highest CO_2/CH_4 selectivity reductions of between 28 and 33% in all the samples (shown in Fig. 3(c), relative to 2008 Robeson's upper bound [60]). Despite this CH_4 permeability increment, the behavior can be explained as swelling-induced perm-selectivity losses, an early stage in polymer plasticization [58].

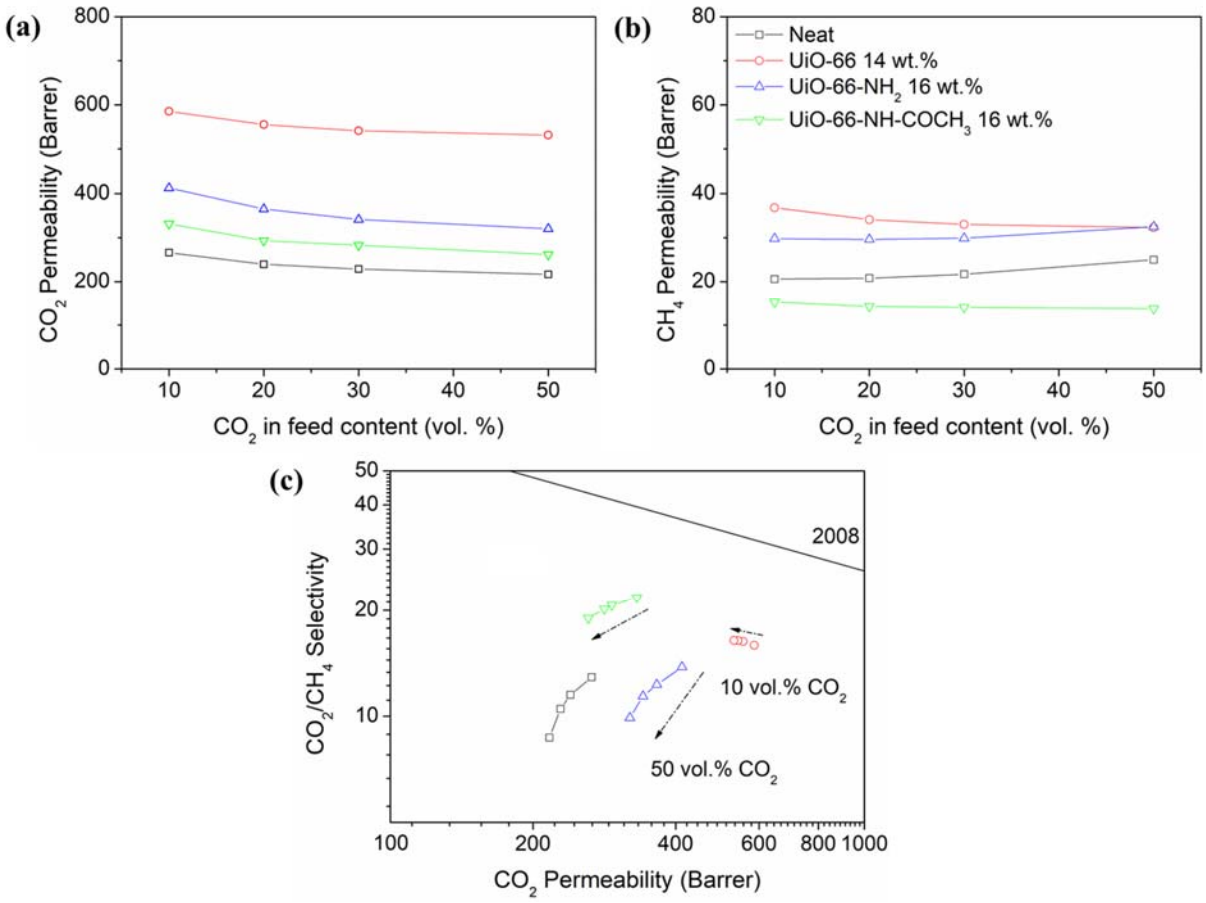

Fig. 3: (a) CO_2 and (b) CH_4 permeabilities of 6FDA-DAM and its respective Zr-MOF MMMs, measured at 20 bar feed pressure and 35 °C. Their corresponding CO_2/CH_4 selectivity values are presented in (c) against 2008 Robeson upper bound [60].

With regard to the initial separation performance (with 10 vol.% CO_2), similarly to the previous discussion, neat 6FDA-DAM showed a lower CO_2/CH_4 selectivity than that of MMMs ($UiO\text{-}66\text{-}NH_2$ < UiO-66 < $UiO\text{-}66\text{-}COCH_3$). The proportional selectivity increase in MMMs to the increasing CO_2 partial pressure [64–66], which only observed in UiO-66 MMM at the tested feed pressure of 20 bar (3% selectivity increment) represents the membrane's extended CO_2 sorption capability due to the CO_2-induced plasticization or swelling at constant pressure [64]. Its reduction conversely was explained based on CO_2 self-inhibition as a consequence of saturation of the filler

active sites at a high CO_2 concentration in a feed mixture [61,67]. Referring to that hypothesis, a lower reduction exhibited by UiO-66-NH-$COCH_3$ MMM (13%) compared to UiO-66-NH_2 MMM (28%), represented by its lesser concave shape in the permeability isotherm, may be due to a higher CO_2 affinity towards acetamide functional groups, with a higher number of adsorption sites compared to UiO-66-NH_2 NPs. Moreover, constant selectivity values demonstrate no dependency of an MMM system towards the increasing CO_2 partial pressure, as also revealed in the PES/SAPO-34/HMA MMM system, measured at 3 bar [61]. This hypothesis implies that only a minor amount of the active sites is occupied at low pressure.

3.3. Effect of operating temperature in the high-pressure separation

Fig. 4(a-c) shows the CO_2 and CH_4 permeability and the CO_2/CH_4 selectivity as a function of the operating temperature applying a 30:70 vol. % CO_2:CH_4 feed mixture at 20 bar. A minor increase in CO_2 permeability of <6% was recorded for all samples, whereas for CH_4 permeability, the increments were higher in between 28 and 37%, as the operating temperature increased from 35 to 55 °C.

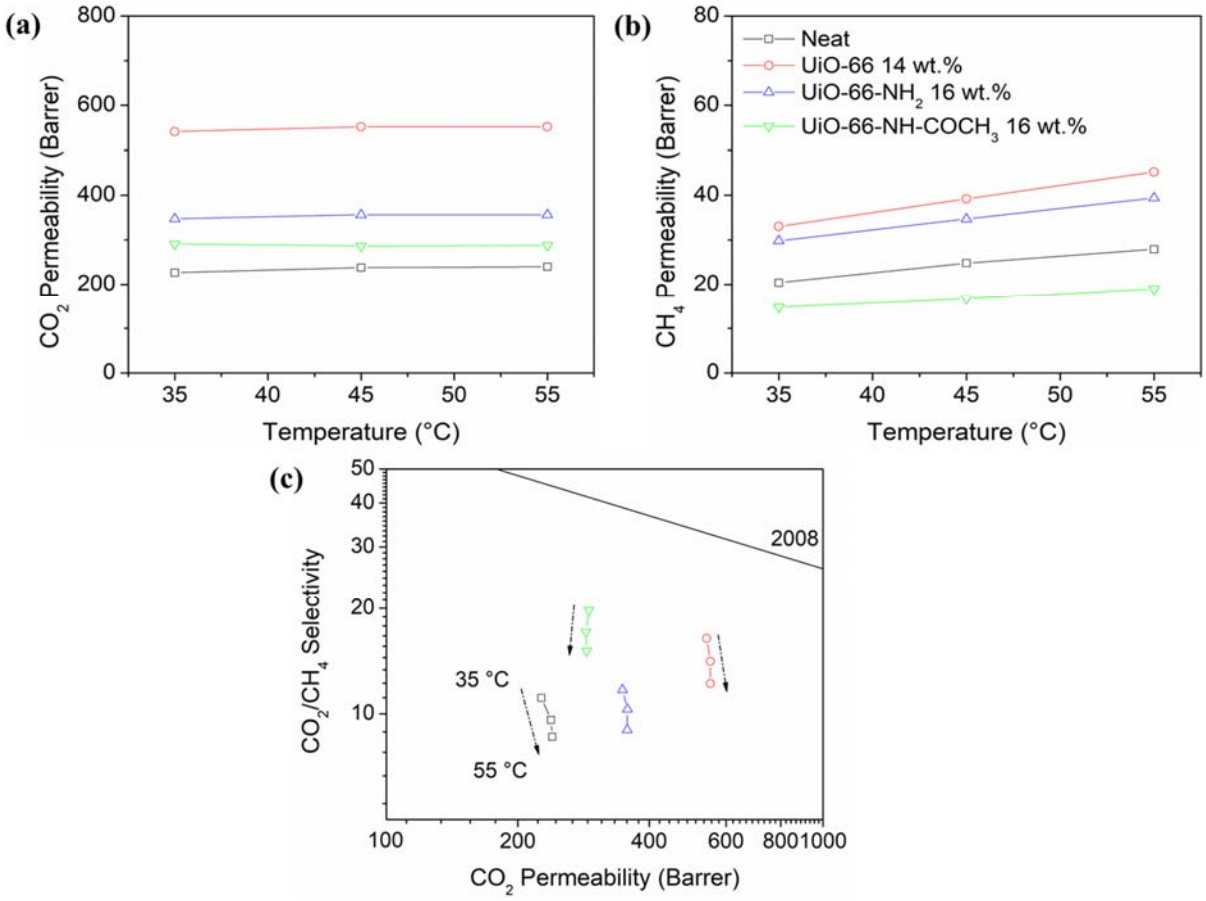

Fig. 4: (a) CO_2 and (b) CH_4 permeabilities of 6FDA-DAM and its respective Zr-MOF MMMs, as a function of temperature with 30:70 vol. % CO_2: CH_4 feed mixture. Data obtained at a feed pressure of 20 bar. Their corresponding (c) CO_2/CH_4 selectivity values are presented against 2008 Robeson upper bound [60].

The effect of temperature on the gas permeability can be quantitatively observed in their activation energy for permeability, following Arrhenius rule using Eq. 3 [68]:

$$P = P_0 e^{\frac{-E_a}{RT}} \quad \text{Eq. 3}$$

Where, P_0 is a pre-exponential factor of permeation, E_a is activation energy for permeability (kJ·mol^{-1}), R is the universal gas constant (8.314 J·mol^{-1}), and T is the temperature in K. Using CO_2/CH_4 selectivity expression of the permeability coefficient ratio of CO_2 over CH_4, the gas selectivity is defined as the following:

$$\alpha(CO_2/CH_4) = \frac{P_{CO2}}{P_{CH4}}$$

$$= \frac{P_0\,(CO_2)}{P_0\,(CH_4)} \exp\left(-\frac{E_p\,(CO_2) - E_p(CH_4)}{RT}\right) \quad \text{...Eq. 4}$$

Fig. S3 indicates that CH_4 permeability (R^2 linear fits of ≥ 0.97) in the 6FDA-DAM neat membrane and its Zr-MOF MMMs followed Arrhenius rule in the temperature range of 35 – 55 °C, while the CO_2 permeability (R^2 linear fits of ≥ 0.48) was less influenced by the temperature and thus shows a large relative error. A lower fit for CO_2 at this high-pressure separation indicated that the molecule's non-ideal behavior in a gas mixture was more influenced by both pressure and temperature, compared to CH_4. The R^2 linear fit for CO_2/CH_4 selectivity was ≥ 0.99. Their permeability coefficients are summarized in **¡Error! No se encuentra el origen de la referencia.**.

Table 2: Activation energy of permeation for CO_2 and CH_4 in neat 6FDA-DAM and its Zr-MOF MMMs, calculated for the temperature operating range of 35 – 55 °C, with 30:70 vol. % CO_2/CH_4 at 20 bar.

Gas	**Membrane**	**Permeability activation energy kJ·mol^{-1}**
		E_a (35 – 55 °C)
CO_2	Neat	0.16
	MMM UiO-66 14 wt.%	0.05
	MMM UiO-66-NH_2 16 wt.%	0.07
	MMM UiO-66-NH-$COCH_3$ 16 wt.%	-0.03
CH_4	Neat	0.85
	MMM UiO-66 14 wt.%	0.86
	MMM UiO-66-NH_2 16 wt.%	0.76
	MMM UiO-66-NH-$COCH_3$ 16 wt.%	0.68

The permeability dependency is a combination of the diffusion and solubility coefficients temperature dependencies, and the lower CO_2 and CH_4 activation energies in MMMs as compared

to the neat polymer indicate gas transport through filler porosity [51]. Regarding 6FDA-DAM, in addition to polymer matrix compression at the high pressure, the overall CO_2 activation energy trend does not show a clear correlation to the membrane FFVs (MMMs (UiO-66; 0.331 > UiO-66-$COCH_3$, 0.292 > UiO-66-NH_2; 0.277) > neat 6FDA-DAM, 0.238). Instead, the activation energy seems profoundly influenced by the presence of Zr-MOF nanoparticles in MMMs, in the order of their group functionalities (UiO-66-NH-$COCH_3$ > UiO-66-NH_2 > UiO-66 > neat 6FDA-DAM). It also concludes that the CO_2 permeation is predominately influenced by its solubility (sorption) in the membrane systems, and less depended on temperature. The higher activation energies presented by the non-polar CH_4 also indicated that its transport was more influenced compared to CO_2 molecules, giving higher CH_4 permeability increments and consequently reduced the CO_2/CH_4 selectivity by 22 – 26%. This observation is consistent with activated diffusion of non-polar molecules in glassy polymers (related to chain mobility and polymer free volumes) [69], where the least permeable gas often possesses a higher activation energy and realizes a more substantial permeability increase with increasing temperature. In any event, the activation energies (temperature-dependent) are low for both the neat polymer membrane and the MMMs, compared to the other 6FDA-based polyimides in the literature (see Table S2). This suggests a low penetrant-membrane interaction perhaps because there is a relatively large difference between the CO_2 and CH_4 kinetic diameter and the membrane controlling pore size.

Besides that, the CH_4 permeability increase was also influenced by the increase of polymer free volume (as a function of polymer chain packing and intersegmental motion) by the effect of elevated temperature. The activated diffusion often proves to be a significant advantage in the separation of non-polar H_2 from CO_2, giving enhanced H_2/CO_2 selectivity at higher temperatures as demonstrated in 6FDA-*m*PBI [69] and PBI-ZIF8 MMMs [70].

$$\log P_0 = \frac{E_p}{R} \times 10^{-3} + Z \quad \text{Eq. 5}$$

Regardless of common polymer chemical structures, Van Krevelen [71] presented a positive slope of 1 x 10^{-3} for log P_0 and E_p/R plot (Eq. 5), with Z values of -7.0 and -8.2 for rubbery and glassy polymers respectively, for permeability measurement below their glass transition temperatures. Fig. S4 indicates that the addition of Zr-MOFs into 6FDA-DAM altered CO_2 permeability-temperature dependency significantly, giving a negative E_p/R slope of -0.15 x 10^{-3}, while only reduced CH_4 permeability-temperature dependency by roughly 70% (CH_4 permeability E_p/R slope = 0.32 x 10^{-3}).

3.4. Effect of the presence of H_2S on membrane separation

The concentration of H_2S in natural gas mixture varies depending on the geo-origin and can be more than 5 vol. % [5,6]. As aforementioned, besides investigating the 6FDA-DAM and its Zr-MOF MMMs performances for H_2S separation, it is important to understand the H_2S effect on membrane performance. We studied the gas separation performance of 6FDA-DAM and its Zr-MOF MMMs with 30:70 vol. % CO_2:CH_4 feed mixture at 20 bar and 35 °C, before switching to 30:5:65 vol. % CO_2:H_2S:CH_4. The separation performance after H_2S exposure were also investigated and summarized in Table 3.

In the presence of 5 vol. % H_2S in the mixed gas, CO_2 permeability in all samples decreased by an average of 28 – 34%, according to their functionality order: MMMs (UiO-66-NH-$COCH_3$ > UiO-66-NH_2 > UiO-66) > neat 6FDA-DAM. Besides the competitive sorption of a two-component gas mixture, the presence of a third component intensifies the gas mixtures non-ideal behavior and influences each penetrant permeation rate, especially at elevated pressures [22]. 6FDA-DAM MMMs showed a higher CO_2 permeability reduction in the presence H_2S, compared to the neat membrane. The observation exhibited the influence of Zr-MOFs addition into the polymer, where

it increased H_2S sorption due to its active metal sites and well-agreed to the order of isosteric adsorption heat in UiO-66 (CO_2; 25.7 kJ·mol^{-1} > H_2S; 23.8 kJ·mol^{-1} > CH_4; 18.8 kJ·mol^{-1}, reported at 30 °C [38]). Functionalized UiO-66 derivatives presented higher values, in the same order. The gas physical properties; dipole moment (Debye), quadrupole moment (au) and polarizability (a_0^3), also greatly contributed to the competitive sorption outcomes and H_2S high polarizability explained its higher permeability despite of its relatively low content in the feed mixture compared to CO_2; CH_4: 5.4 x 10-6 Debye, 0 au, 17.3 a_0^3; CO_2: 0 Debye, 3.2 au, 18 a_0^3; H_2S: 0.978 Debye, 0 au, 25 a_0^3 [72]. Hence, the observed CO_2/CH_4 selectivity reduction can be explained by a larger competitive sorption effect induced by H_2S, as the solubility of H_2S is larger than that of CH_4 in the membrane systems. Furthermore, the effect on selectivity reduction was proven to be more prominent in the neat membranes (-30%) compared to the 6FDA-DAM Zr-MOFs MMMs (-17 – 19%).

In the presence of H_2S, all MMMs presented higher CO_2/CH_4 and H_2S/CH_4 selectivities compared to the neat 6FDA-DAM ($\alpha_{CO2/CH4}$ = 9.1; $\alpha_{H2S/CH4}$ = 7.4) with the highest values presented in UiO-66-NH-$COCH_3$ MMM ($\alpha_{CO2/CH4}$ = 18.2; $\alpha_{H2S/CH4}$ = 16.2). The UiO-66-NH-$COCH_3$ MMM presented similar or higher H_2S/CH_4 selectivity than several membranes, such as in 6FDA-PAI-3/TmPDA (ideal $\alpha_{H2S/CH4}$ = 10.9) and Torlon® 4000T (ideal $\alpha_{H2S/CH4}$ = 14.8), both tested at 4.5 bar, 35 °C [73], and in a rigid (6FDA-mPDA)-(6FDA-durene) block co-polyimide, ($\alpha_{H2S/CH4}$ = ca. 15), when tested with 1 vol. % H_2S in a CO_2:H_2S:N_2:CH_4 quaternary mixture at 3.8 bar, 22 °C [74]. The performance is also comparable to the commercial poly(ester urethane) urea, PEUU, $\alpha_{H2S/CH4}$ = 16 [75] (CO_2:H_2S:CH_4 feed ratio of 5.4:3:remaining, at 55 °C, 20 bar) and cellulose acetate, CA, $\alpha_{H2S/CH4}$ = 19 [76] (CO_2:H_2S:CH_4 feed ratio of 29:6:65, at 35 °C, 10 bar). In the separation of an actual natural gas sample containing 5008 ppm H_2S, water vapor, C_1-*n*C_5, and mercaptan,

commercial polyphenylene oxide hollow fibers presented $\alpha_{H2S/CH4}$ = 2.9, while a commercial poly (ester urethane) urea (PEUU) flat sheet membrane gave $\alpha_{H2S/CH4}$ = 3.4, measured at 40 °C and 23 °C, respectively [77]. The separation performances of several other dense membranes to the ternary gas mixture with H_2S at 35 °C are presented in Table S3 for comparison.

Table 3: Gas separation performances of 6FDA-DAM and its 14 – 16 wt.% Zr-MOFs MMMs, tested with binary (30:70 vol.%; CO_2: CH_4) and tertiary (30:5:65 vol.%; CO_2: H_2S: CH_4) feed mixture at 20 bar, 35 °C.

Feed mixture	**Separation performances**	**6FDA-DAM membranes**			
		Neat	MMM UiO-66	MMM UiO-66-NH_2	MMM UiO-66-NH-$COCH_3$
CO_2:CH_4 (30:70 vol. %) Before exposure	Gas permeability (Barrer)				
	CO_2	231	541	359	291
	CH_4	21.7	33.0	33.1	14.8
	CO_2/CH_4 selectivity	10.6	16.4	10.8	19.7
CO_2:H_2S:CH_4 (30:5:65 vol. %)	Gas permeability (Barrer)				
	CO_2	167	385	243	193
	H_2S	137	352	224	172
	CH_4	18.5	25.4	25.7	10.6
	CO_2/CH_4 selectivity	9.1	15.2	9.5	18.2
	H_2S/CH_4 selectivity	7.4	13.6	8.7	16.2
CO_2:CH_4 (30:70 vol. %) After exposure	Gas permeability (Barrer)				
	CO_2	227	543	347	284
	CH_4	20.4	33.7	29.8	14.3
	CO_2/CH_4 selectivity	11.1	16.1	11.7	19.8

Interestingly, after the H_2S exposure for a period of 20 – 40 h, both CO_2 permeability and CO_2/CH_4 selectivity of all membranes were regained to pre-H_2S exposure values, indicating the presence of H_2S only caused a reversible competitive sorption between the permeating molecules and no H_2S-induced plasticization or other permanent effect. These remarkable results confirmed the capability of polymer 6FDA-DAM and its Zr-MOF MMMs for simultaneous acid gases (CO_2, H_2S) separation from CH_4.

4.0. CONCLUSION

6FDA-DAM co-polyimide offers an attractive opportunity in gas separation application, and the incorporation of the highly stable zirconium-based UiO-66 and its functionalized derivatives as MMM further enhanced the separation properties. The membranes possessed excellent CO_2/CH_4 separation performance and presented high-performance stability at conditions relevant to actual gas processing (pressure, CO_2 content, temperature). The Zr-MOFs improved not only 6FDA-DAM gas separation properties but also deterred CO_2-induced plasticization and swelling. Additionally, in the presence of high H_2S content (50,000 ppm in feed mixture) at high total pressure, both CO_2- and H_2S-induced plasticization were suppressed and only reversible competitive sorption effect was observed. This successful high-pressure testing of 6FDA-DAM MMMs with Zr-MOFs is encouraging and industrially relevant for natural gas sweetening at high pressure. Nevertheless, the separation understanding in the presence of water vapor and condensable hydrocarbons needs to be addressed beforehand. These impurities are not only suspected to reduce the separation performance but could also deteriorate the physical integrity of a membrane system.

Acknowledgements

The research leading to these results has received funding from ECCSEL (Grant Agreement no. 675206, European Union's Horizon 2020 research and innovation programme). The authors also acknowledge the financial support of EACEA/European Commission, within the "Erasmus Mundus Doctorate in Membrane Engineering – EUDIME" (ERASMUS MUNDUS Programme 2009-2013, FPA n. 2011-0014, SGA n. 2012-1719), the Spanish Ministry of Economy and Competitiveness (MINECO), FEDER (MAT2016-77290-R), the European Social Fund and the Aragón Government (DGA, T05).

References

[1] S. Faramawy, T. Zaki, A.A.E. Sakr, Natural gas origin, composition, and processing: A review, J. Nat. Gas Sci. Eng. 34 (2016) 34–54. doi:10.1016/j.jngse.2016.06.030.

[2] V.A. Skorobogatov, V.S. Yakushev, E.M. Chuvillin, Sources of natural gas within permafrost North-West Siberia, in: Permafr. - Sevent Int. Conf., 1998: pp. 1001–1007.

[3] B. Shimekit, H. Mukhtar, Natural Gas Purification Technologies–Major Advances for CO2 Separation and Future Directions, Adv. Nat. Gas Technol. (2012) 235–270. doi:10.5772/38656.

[4] X.Y. Chen, H. Vinh-Thang, A.A. Ramirez, D. Rodrigue, S. Kaliaguine, Membrane gas separation technologies for biogas upgrading, RSC Adv. 5 (2015) 24399–24448. doi:10.1039/C5RA00666J.

[5] A. Kazemi, M. Malayeri, A. Gharibi kharaji, A. Shariati, Feasibility study, simulation and economical evaluation of natural gas sweetening processes - Part 1: A case study on a low capacity plant in iran, J. Nat. Gas Sci. Eng. 20 (2014) 16–22. doi:10.1016/j.jngse.2014.06.001.

[6] A. Kazemi, A.G. Kharaji, A. Mehrabani-Zeinabad, V. Faizi, J. Kazemi, A. Shariati, Synergy between two natural gas sweetening processes, J. Unconv. Oil Gas Resour. 14 (2016) 6–11. doi:10.1016/j.juogr.2016.01.002.

[7] Z.A. Manan, W.N.R. Mohd Nawi, S.R. Wan Alwi, J.J. Klemeš, Advances in Process Integration research for CO 2 emission reduction – A review, J. Clean. Prod. 167 (2017) 1–13. doi:10.1016/j.jclepro.2017.08.138.

[8] E.D. Bates, R.D. Mayton, I. Ntai, J.H. Davis, CO2 capture by a task-specific ionic liquid, J. Am. Chem. Soc. 124 (2002) 926–927. doi:10.1021/ja017593d.

[9] A.J. Kidnay, W.R. Parrish, Overview of natural gas industry, in: L.L. Faulkner (Ed.), Fundam. Nat. Gas Process., CRC Press, Taylor & Francis Group, Boca Raton, FL, 2006: pp. 1–21.

[10] M. Galizia, W.S. Chi, Z.P. Smith, T.C. Merkel, R.W. Baker, B.D. Freeman, 50th Anniversary

Perspective : Polymers and Mixed Matrix Membranes for Gas and Vapor Separation : A Review and Prospective Opportunities, Macromolecules. (2017) 7809–7843. doi:10.1021/acs.macromol.7b01718.

[11] R.W. Baker, Vapor and Gas Separation by Membranes, in: Adv. Membr. Technol. Appl., John Wiley & Sons, Inc., 2008: pp. 557–580. doi:10.1002/9780470276280.ch21.

[12] T. Rodenas, I. Luz, G. Prieto, B. Seoane, H. Miro, A. Corma, F. Kapteijn, F.X. Llabrés i Xamena, J. Gascon, Metal–organic framework nanosheets in polymer composite materials for gas separation, Nat. Mater. 14 (2014) 48–55. doi:10.1038/nmat4113.

[13] R.W. Baker, K. Lokhandwala, Natural gas processing with membranes: An overview, Ind. Eng. Chem. Res. 47 (2008) 2109–2121. doi:10.1021/ie071083w.

[14] N.L. Le, Y. Wang, T.S. Chung, Synthesis, cross-linking modifications of 6FDA-NDA/DABA polyimide membranes for ethanol dehydration via pervaporation, J. Memb. Sci. 415–416 (2012) 109–121. doi:10.1016/j.memsci.2012.04.042.

[15] K. Vanherck, G. Koeckelberghs, I.F.J. Vankelecom, Crosslinking polyimides for membrane applications: A review, Prog. Polym. Sci. 38 (2013) 874–896. doi:10.1016/j.progpolymsci.2012.11.001.

[16] J.D. Wind, C. Staudt-Bickel, D.R. Paul, W.J. Koros, Solid-state covalent cross-linking of polyimide membranes for carbon dioxide plasticization reduction, Macromolecules. 36 (2003) 1882–1888. doi:10.1021/ma025938m.

[17] M.L. Chua, Y.C. Xiao, T.S. Chung, Modifying the molecular structure and gas separation performance of thermally labile polyimide-based membranes for enhanced natural gas purification, Chem. Eng. Sci. 104 (2013) 1056–1064. doi:10.1016/j.ces.2013.10.034.

[18] W.F. Yong, K.H.A. Kwek, K.S. Liao, T.S. Chung, Suppression of aging and plasticization in highly permeable polymers, Polym. (United Kingdom). 77 (2015) 377–386. doi:10.1016/j.polymer.2015.09.075.

[19] R.T. Adams, J.S. Lee, T.H. Bae, J.K. Ward, J.R. Johnson, C.W. Jones, S. Nair, W.J. Koros, CO2-CH4 permeation in high zeolite 4A loading mixed matrix membranes, J. Memb. Sci. 367 (2011) 197–203. doi:10.1016/j.memsci.2010.10.059.

[20] S. Shahid, K. Nijmeijer, High pressure gas separation performance of mixed-matrix polymer membranes containing mesoporous Fe(BTC), J. Memb. Sci. 459 (2014) 33–44. doi:10.1016/j.memsci.2014.02.009.

[21] S. Akbar, A.H. Navarchian, Separation of carbon dioxide from natural gas through Matrimid-based mixed matrix membranes, Gas Process. J. 4 (2016) 1–18. doi:10.22108/gpj.2017.102840.1009.

[22] T. Visser, G.H. Koops, M. Wessling, On the subtle balance between competitive sorption and

plasticization effects in asymmetric hollow fiber gas separation membranes, J. Memb. Sci. 252 (2005) 265–277. doi:10.1016/j.memsci.2004.12.015.

[23] S. Lee, M. Binns, J.H. Lee, J.-H. Moon, J. Yeo, Y.-K. Yeo, Y.M. Lee, J.-K. Kim, Membrane Separation Process for {CO2} Capture from Mixed Gases using {TR} and {XTR} Hollow Fiber Membranes: Process Modeling and Experiments, J. Memb. Sci. 541 (2017). doi:https://doi.org/10.1016/j.memsci.2017.07.003.

[24] M. Scholz, T. Harlacher, T. Melin, M. Wessling, Modeling gas permeation by linking nonideal effects, Ind. Eng. Chem. Res. 52 (2013) 1079–1088. doi:10.1021/ie202689m.

[25] C.A. Scholes, G.W. Stevens, S.E. Kentish, The effect of hydrogen sulfide, carbon monoxide and water on the performance of a PDMS membrane in carbon dioxide/nitrogen separation, J. Memb. Sci. 350 (2010) 189–199. doi:10.1016/j.memsci.2009.12.027.

[26] M. Saberi, A.A. Dadkhah, S.A. Hashemifard, Modeling of simultaneous competitive mixed gas permeation and CO2 induced plasticization in glassy polymers, J. Memb. Sci. 499 (2016) 164–171. doi:10.1016/j.memsci.2015.09.044.

[27] O.M. Yaghi, M. O'Keeffe, N.W. Ockwig, H.K. Chae, M. Eddaoudi, J. Kim, Reticular synthesis and the design of new materials, Nature. 423 (2003) 705–714. doi:10.1038/nature01650.

[28] H.B. Tanh Jeazet, C. Staudt, C. Janiak, Metal–organic frameworks in mixed-matrix membranes for gas separation, Dalt. Trans. 41 (2012) 14003. doi:10.1039/c2dt31550e.

[29] X. Yan, S. Komarneni, Z. Zhang, Z. Yan, Extremely enhanced CO2 uptake by HKUST-1 metal-organic framework via a simple chemical treatment, Microporous Mesoporous Mater. 183 (2014) 69–73. doi:10.1016/j.micromeso.2013.09.009.

[30] A.R. Millward, O.M. Yaghi, Metal-organic frameworks with exceptionally high capacity for storage of carbon dioxide at room temperature, J. Am. Chem. Soc. 127 (2005) 17998–17999. doi:10.1021/ja0570032.

[31] O.K. Farha, I. Eryazici, N.C. Jeong, B.G. Hauser, C.E. Wilmer, A.A. Sarjeant, R.Q. Snurr, S.T. Nguyen, A.Ö. Yazaydin, J.T. Hupp, Metal-organic framework materials with ultrahigh surface areas: Is the sky the limit?, J. Am. Chem. Soc. 134 (2012) 15016–15021. doi:10.1021/ja3055639.

[32] E. Adatoz, A.K. Avci, S. Keskin, Opportunities and challenges of MOF-based membranes in gas separations, Sep. Purif. Technol. 152 (2015) 207–237. doi:10.1016/j.seppur.2015.08.020.

[33] M. Zamidi Ahmad, M. Navarro, M. Lhotka, B. Zornoza, C. Téllez, V. Fila, J. Coronas, Enhancement of CO2/CH4 separation performances of 6FDA-based co-polyimides mixed matrix membranes embedded with UiO-66 nanoparticles, Sep. Purif. Technol. 192 (2018) 465–474. doi:https://doi.org/10.1016/j.seppur.2017.10.039.

[34] V. Martin-Gil, A. Lopez, P. Hrabanek, R. Mallada, I.F.J. Vankelecom, V. Fila, Study of different

titanosilicate (TS-1 and ETS-10) as fillers for Mixed Matrix Membranes for CO2/CH4 gas separation applications, J. Memb. Sci. 523 (2017) 24–35. doi:10.1016/j.memsci.2016.09.041.

[35] E.M. Mahdi, J.C. Tan, Mixed-matrix membranes of zeolitic imidazolate framework (ZIF-8)/Matrimid nanocomposite: Thermo-mechanical stability and viscoelasticity underpinning membrane separation performance, J. Memb. Sci. 498 (2016) 276–290. doi:10.1016/j.memsci.2015.09.066.

[36] M.Z. Ahmad, M. Navarro, M. Lhotka, B. Zornoza, C. Téllez, W.M. De Vos, N.E. Benes, N.M. Konnertz, T. Visser, R. Semino, Enhanced gas separation performance of 6FDA-DAM based mixed matrix membranes by incorporating MOF UiO-66 and its derivatives, J. Memb. Sci. 558 (2018) 64–77. doi:10.1016/j.memsci.2018.04.040.

[37] R. Semino, J.C. Moreton, N.A. Ramsahye, S.M. Cohen, G. Maurin, Understanding the origins of metal–organic framework/polymer compatibility, Chem. Sci. 00 (2018) 1–10. doi:10.1039/C7SC04152G.

[38] Z. Li, F. Liao, F. Jiang, B. Liu, S. Ban, G. Chen, C. Sun, P. Xiao, Y. Sun, Capture of H2S and SO2 from trace sulfur containing gas mixture by functionalized UiO-66(Zr) materials: A molecular simulation study, Fluid Phase Equilib. 427 (2016) 259–267. doi:10.1016/j.fluid.2016.07.020.

[39] M.W. Anjum, F. Vermoortele, A.L. Khan, B. Bueken, D.E. De Vos, I.F.J. Vankelecom, Modulated UiO-66-Based Mixed-Matrix Membranes for CO2 Separation, ACS Appl. Mater. Interfaces. 7 (2015) 25193–25201. doi:10.1021/acsami.5b08964.

[40] L. Hou, L. Wang, N. Zhang, Z. Xie, D. Dong, Polymer brushes on metal-organic frameworks by UV-induced photopolymerization, Polym. Chem. 7 (2016) 5828–5834. doi:10.1039/C6PY01008C.

[41] S.J. Garibay, S.M. Cohen, Isoreticular synthesis and modification of frameworks with the UiO-66 topology., Chem. Commun. (Camb). 46 (2010) 7700–2. doi:10.1039/c0cc02990d.

[42] S. Basu, A. Cano-Odena, I.F.J. Vankelecom, MOF-containing mixed-matrix membranes for CO2/CH4 and CO2/N2 binary gas mixture separations, Sep. Purif. Technol. 81 (2011) 31–40. doi:10.1016/j.seppur.2011.06.037.

[43] S.A. Hashemifard, A.F. Ismail, T. Matsuura, Prediction of gas permeability in mixed matrix membranes using theoretical models, J. Memb. Sci. 347 (2010) 53–61. doi:10.1016/j.memsci.2009.10.005.

[44] P.S. Goh, A.F. Ismail, S.M. Sanip, B.C. Ng, M. Aziz, Recent advances of inorganic fillers in mixed matrix membrane for gas separation, Sep. Purif. Technol. 81 (2011) 243–264. doi:10.1016/j.seppur.2011.07.042.

[45] A. Perea-Cachero, J. Sánchez-Laínez, Á. Berenguer-Murcia, D. Cazorla-Amorós, C. Téllez, J. Coronas, A new zeolitic hydroxymethylimidazolate material and its use in mixed matrix membranes

based on 6FDA-DAM for gas separation, J. Memb. Sci. 544 (2017) 88–97. doi:10.1016/j.memsci.2017.09.009.

[46] B.D. Freeman, Basis of Permeability/Selectivity Tradeoff Relations in Polymeric Gas Separation Membranes, Macromolecules. 32 (1999) 375–380. doi:10.1021/ma9814548.

[47] S. Shahid, K. Nijmeijer, Performance and plasticization behavior of polymer-MOF membranes for gas separation at elevated pressures, J. Memb. Sci. 470 (2014) 166–177. doi:10.1016/j.memsci.2014.07.034.

[48] B. Zornoza, C. Tellez, J. Coronas, J. Gascon, F. Kapteijn, Metal organic framework based mixed matrix membranes: An increasingly important field of research with a large application potential, Microporous Mesoporous Mater. 166 (2013) 67–78. doi:10.1016/j.micromeso.2012.03.012.

[49] H. Lin, M. Yavari, Upper bound of polymeric membranes for mixed-gas CO2/CH4 separations, J. Memb. Sci. 475 (2015) 101–109. doi:10.1016/j.memsci.2014.10.007.

[50] O.G. Nik, X.Y. Chen, S. Kaliaguine, Functionalized metal organic framework-polyimide mixed matrix membranes for CO 2/CH 4 separation, J. Memb. Sci. 413–414 (2012) 48–61. doi:10.1016/j.memsci.2012.04.003.

[51] S. Castarlenas, C. Tellez, J. Coronas, Gas separation with mixed matrix membranes obtained from MOF UiO-66-graphite oxide hybrids, J. Memb. Sci. 526 (2017) 205–211. doi:10.1016/j.memsci.2016.12.041.

[52] V. Stannett, The transport of gases in synthetic polymeric membranes - an historic perspective, J. Memb. Sci. 3 (1978) 97–115. doi:10.1016/S0376-7388(00)83016-1.

[53] J.E. Bachman, J.R. Long, Plasticization-resistant Ni $_2$ (dobdc)/polyimide composite membranes for the removal of CO $_2$ from natural gas, Energy Environ. Sci. 9 (2016) 2031–2036. doi:10.1039/C6EE00865H.

[54] J.E. Bachman, Z.P. Smith, T. Li, T. Xu, J.R. Long, Enhanced ethylene separation and plasticization resistance in polymer membranes incorporating metal–organic framework nanocrystals, Nat. Mater. 15 (2016) 845–849. doi:10.1038/nmat4621.

[55] B. Zornoza, C. Téllez, J. Coronas, O. Esekhile, W.J. Koros, Mixed matrix membranes based on 6FDA polyimide with silica and zeolite microsphere dispersed phases, AIChE J. 61 (2015) 4481–4490. doi:10.1002/aic.15011.

[56] J.D. Wind, C. Staudt-Bickel, D.R. Paul, W.J. Koros, The Effects of Crosslinking Chemistry on CO $_2$ Plasticization of Polyimide Gas Separation Membranes, Ind. Eng. Chem. Res. 41 (2002) 6139–6148. doi:10.1021/ie0204639.

[57] R. Heck, M.S. Qahtani, G.O. Yahaya, I. Tanis, D. Brown, A.A. Bahamdan, A.W. Ameen, M.M. Vaidya, J.P.R. Ballaguet, R.H. Alhajry, E. Espuche, R. Mercier, Block copolyimide membranes for

pure- and mixed-gas separation, Sep. Purif. Technol. 173 (2017) 183–192. doi:10.1016/j.seppur.2016.09.024.

[58] R. Swaidan, B. Ghanem, E. Litwiller, I. Pinnau, Effects of hydroxyl-functionalization and sub-Tg thermal annealing on high pressure pure- and mixed-gas CO2/CH4 separation by polyimide membranes based on 6FDA and triptycene-containing dianhydrides, J. Memb. Sci. 475 (2015) 571–581. doi:10.1016/j.memsci.2014.10.046.

[59] W.J. Koros, R.T. Chern, V. Stannett, H.B. Hopfenberg, A model for permeation of mixed gases and vapors in glassy polymers, J. Polym. Sci. Polym. Phys. Ed. 19 (1981) 1513–1530. doi:10.1002/pol.1981.180191004.

[60] L.M. Robeson, The upper bound revisited, J. Memb. Sci. 320 (2008) 390–400. doi:10.1016/j.memsci.2008.04.030.

[61] U. Cakal, L. Yilmaz, H. Kalipcilar, Effect of feed gas composition on the separation of CO 2/CH 4 mixtures by PES-SAPO 34-HMA mixed matrix membranes, J. Memb. Sci. 417–418 (2012) 45–51. doi:10.1016/j.memsci.2012.06.011.

[62] J.H. Kim, W.J. Koros, D.R. Paul, Effects of CO2 exposure and physical aging on the gas permeability of thin 6FDA-based polyimide membranes. Part 1. Without crosslinking, J. Memb. Sci. 282 (2006) 21–31. doi:10.1016/j.memsci.2006.05.004.

[63] L. Cui, W. Qiu, D.R. Paul, W.J. Koros, Responses of 6FDA-based polyimide thin membranes to CO2 exposure and physical aging as monitored by gas permeability, Polymer (Guildf). 52 (2011) 5528–5537. doi:10.1016/j.polymer.2011.10.008.

[64] S. Sridhar, B. Smitha, T.M. Aminabhavi, Separation of carbon dioxide from natural gas mixtures through polymeric membranes - A review, Sep. Purif. Rev. 36 (2007) 113–174. doi:10.1080/15422110601165967.

[65] E. V. Perez, K.J. Balkus, J.P. Ferraris, I.H. Musselman, Mixed-matrix membranes containing MOF-5 for gas separations, J. Memb. Sci. 328 (2009) 165–173. doi:10.1016/j.memsci.2008.12.006.

[66] A. Bos, I.G.M. Pünt, M. Wessling, H. Strathmann, CO2-induced plasticization phenomena in glassy polymers, J. Memb. Sci. 155 (1999) 67–78. doi:10.1016/S0376-7388(98)00299-3.

[67] T. Battal, N. Baç, L. Yilmaz, Effect of Feed Composition on the Performance of Polymer-Zeolite Mixed Matrix Gas Separation Membranes, Sep. Sci. Technol. 30 (1995) 2365–2384. doi:10.1080/01496399508013117.

[68] T. Komatsuka, K. Nagai, Temperature Dependence on Gas Permeability and Permselectivity of Poly(lactic acid) Blend Membranes, Polym. J. 41 (2009) 455–458. doi:10.1295/polymj.PJ2008266.

[69] R.P. Singh, X. Li, K.W. Dudeck, B.C. Benicewicz, K.A. Berchtold, Polybenzimidazole based random copolymers containing hexafluoroisopropylidene functional groups for gas separations at

elevated temperatures, Polymer (Guildf). 119 (2017) 134–141. doi:10.1016/j.polymer.2017.04.075.

[70] J. Sánchez-Laínez, B. Zornoza, S. Friebe, J. Caro, S. Cao, A. Sabetghadam, B. Seoane, J. Gascon, F. Kapteijn, C. Le Guillouzer, G. Clet, M. Daturi, C. Téllez, J. Coronas, Influence of ZIF-8 particle size in the performance of polybenzimidazole mixed matrix membranes for pre-combustion CO2 capture and its validation through interlaboratory test, J. Memb. Sci. 515 (2016) 45–53. doi:10.1016/j.memsci.2016.05.039.

[71] D.W. Van Krevelen, K. Te Nijenhuis, Chapter 7 - Cohesive Properties and Solubility, in: D.W. Van Krevelen, K. Te Nijenhuis (Eds.), Prop. Polym. (Fourth Ed., Fourth Edi, Elsevier, Amsterdam, 2009: pp. 189–227. doi:https://doi.org/10.1016/B978-0-08-054819-7.00007-8.

[72] A.A. Radzig, B.M. Smirnov, Interaction Potentials Between Atomic and Molecular Species, in: Ref. Data Atoms, Mol. Ions. Springer Ser. Chem. Phys., Springer, Berlin, Heidelberg, 1985: pp. 317–315. doi:https://doi.org/10.1007/978-3-642-82048-9_9.

[73] J. Vaughn, W.J. Koros, Effect of the Amide Bond Diamine Structure on the CO 2 , H 2 S, and CH 4 Transport Properties of a Series of Novel 6FDA-Based Polyamide–Imides for Natural Gas Purification, Macromolecules. 45 (2012) 7036–7049. doi:10.1021/ma301249x.

[74] G.O. Yahaya, M.S. Qahtani, A.Y. Ammar, A.A. Bahamdan, A.W. Ameen, R.H. Alhajry, M.M.B. Sultan, F. Hamad, Aromatic block co-polyimide membranes for sour gas feed separations, Chem. Eng. J. 304 (2016) 1020–1030. doi:10.1016/j.cej.2016.06.076.

[75] T. Mohammadi, M.T. Moghadam, M. Saeidi, M. Mahdyarfar, Acid gas permeation behavior through poly (ester urethane urea) membrane, Ind. Eng. Chem. Res. 47 (2008) 7361–7367.

[76] G. Chatterjee, A.A. Houde, S.A. Stern, Poly(ether urethane) and poly(ether urethane urea) membranes with high H2S/CH4 selectivity, J. Memb. Sci. 135 (1997) 99–106. doi:10.1016/S0376-7388(97)00134-8.

[77] S.M.S. Niknejad, H. Savoji, M. Pourafshari Chenar, M. Soltanieh, Separation of H2S from CH4 by polymeric membranes at different H2S concentrations, Int. J. Environ. Sci. Technol. 14 (2017) 375–384. doi:10.1007/s13762-016-1156-3.